17th Australasian Fluid Mechanics Conference
Auckland, New Zealand
5-9 December 2010

Steady Aerodynamics of Rod and Plate Type Debris

P.J. Richards[1]

[1]Department of Mechanical Engineering
University of Auckland, Auckland 1142, New Zealand

Abstract

Windborne debris causes extensive damage to buildings and other structures during extreme wind storms. In order to understand the damage potential of such debris it is desirable to be able to model their flight behaviours. Such trajectories generally involve full 6 degree-of-freedom motion. In order to facilitate such analysis steady forces and moments have been measured on three plate and three rod geometries which represent generic examples of windborne debris. It is shown that these forces and moments are complex functions of the angle of attack, the tilt angle and the geometry. With plates some of the characteristics can be related to the effective aspect ratio for a particular orientation. Methods for transferring the data into a trajectory program and allowing interpolation are outlined.

Introduction

During extreme storms, such as tropical cyclones, many buildings are initially damaged by windborne debris. Breakage of windows or doors can then lead to internal pressurisation and possible loss of roofs. Such failures generate further debris which damages more buildings downstream. It is hence important to consider what types of debris are likely to occur, what are their likely masses, how far they are likely to travel and what fraction of the wind speed they are likely to attain before impact. In order to do this appropriate models for the aerodynamic forces and moments are required. Willis et al. [18] provide a useful classification system of debris into compact objects, with all three dimension of a similar scale, plate (or sheet) type objects with one dimension much smaller than the other two and rod type objects with one dimension larger than the other two.

Holmes [4] has considered the trajectories of compact objects, but recognises that this is the simplest type of object to consider since only the drag force is relevant and hence the only aerodynamic data required is the drag coefficient. Since these are readily available in the literature compact debris will not be considered further in this paper.

Plate type debris has been considered by a number of authors [1,2,5,6,9-11,14-17]. Although some of the experimental results show the motions to be three dimensional (see for example Visscher and Kopp [16]), most of the trajectory models used have only considered the two dimensional situations where one of the axes of symmetry of rectangular plates lies in the plane of motion. In such 2D cases the only aerodynamic data required is the normal force coefficient and the centre of pressure location as a function of the angle of attack. The most frequently used data is that for a square plate obtain by Flachsbart [7] and reported by Hoerner[3]. Very similar data is reported by Holmes et al. [6] from a number of sources. However this data is restricted to plane motion where one edge of the plate remains perpendicular to the plane of motion.

Although rod type debris, such a roof frame timbers, is quite common there has been relatively little research related to rod type debris, Tachikawa and Hara [13] measured the force coefficients of several rectangular cylinders and Lin et al. [8] report the trajectories of rod-like debris, but even these were always released with the wind parallel to one plane of symmetry and so the resulting trajectories are planar. It is only Tachikawa [15] who has experimentally studied the three-dimensional motion of both sheet and rod type debris. However, it is this three dimensional motion that is most likely to occur in real situations.

While 2-dimensional trajectory models can demonstrate many basic principles, planar motion is a special case that is unlikely to occur in a real storm situation. In these simplified cases the force coefficients and the position of the centre of pressure on each face are only functions of the angle of attack. In addition the centre of pressure is always located on the plane of symmetry. However the real situation is significantly more complex.

Wind tunnel measurements at the University of Auckland, for both plate and rod type debris, have sought to provide force and moment information for more general situations including all possible orientations of several generic shapes. Richards et al. [12] present wind tunnel measurement of the forces acting on plates with aspect ratios of 1, 2 and 4 at a wide range of orientations representing most possible angles in general 6 degree-of-freedom flight. They show that while the square plate data is very similar to that reported by other researchers the other plates demonstrated strong asymmetries depending on orientation. In addition force data was obtained for rods 1.5m long and 45mm thick but with widths of 45, 90 and 135mm. While these data show some interesting behaviours it was recognised that the angular increment used in these tests was quite coarse and that the remote force balance used could not reliably measure the moments applied to the rods. As a consequence new wind tunnel measurements have been conducted for both plates and rods using a JR3 force balance with the objects directly attached to the balance. These new measurements provide both force and moment data at angle of attack intervals of 5º and tilt angle intervals of 15º.

It is recognised that these aerodynamic force and moment measurements are for a steady situation, whereas in free flight these will be modified by rotation of the plate or rod. However in the early stages of a flight the projectile will probably only be rotating slowly and it is during this period that the relative velocity is at its maximum and hence the forces and moments are most significant. It is therefore suggested that such steady forces and moments may be used in the early stages of a trajectory although rotational affect would need to be taken into account in the later stages of a flight.

Wind Tunnel Testing

The steady force and moment measurements were conducted in the University of Auckland's "Twisted Flow Wind Tunnel". This tunnel is specifically designed to create the twisted flow encountered by a moving yacht; however for the current tests the turning vanes were moved to the side and can just be seen on the right of Figure 1(a). The wind tunnel is normally 7m wide and

3.5m high, but for these tests contractions were use in order to reduce the width to 3.5m. Since the maximum blockage ratio was only 2% and it is an open jet tunnel no blockage corrections have been made. The mean wind speed used was 7.5 m/s. The plates and rods were mounted directly onto the JR3 6-component balance which was help by a central pivot at the top of a 1.3m high post. For the earlier testing [12] the sub-floor 6 component force balance was used but in the current tests this balance was only used for spot checks. During testing the floor level support structure was covered by a false floor, which shielded it from the wind. The angle of attack (α, see Figure 1(b)) was varied by rotating the complete setup on the turntable. The zero crossing of the normal force has been used to correct for small angular misalignments. The tilt angle (γ) was varied by rotating the plate or rod and the JR3 balance about a horizontal axis.

Due to the limited load capacity of the JR3 balance the weight of the plates and rods had to be restricted. In order to achieve this 7mm plywood sheets were used. Each plate had an area of $0.25m^2$ but the side length ratios (SR) were 1, 2 and 4. For the rods a hardboard and polystyrene foam sandwich was used in order to keep the weight low while providing sufficient stiffness. All rods were 1.5m long and 45mm thick, while the widths were 45, 90 and 135mm.

The axis system used in this paper has the X axis perpendicular to the largest face and the Z axis along the largest dimension. For the plates the side length ratio $SR=\ell_z/\ell_y$ while the thickness ℓ_x=7mm is constant, whereas for rods the cross-section ratio $CSR=\ell_y/\ell_x$ while the length ℓ_z=1.5m is fixed. The force and moment coefficients have been calculated by using the largest face area and largest dimension as normalising parameters.

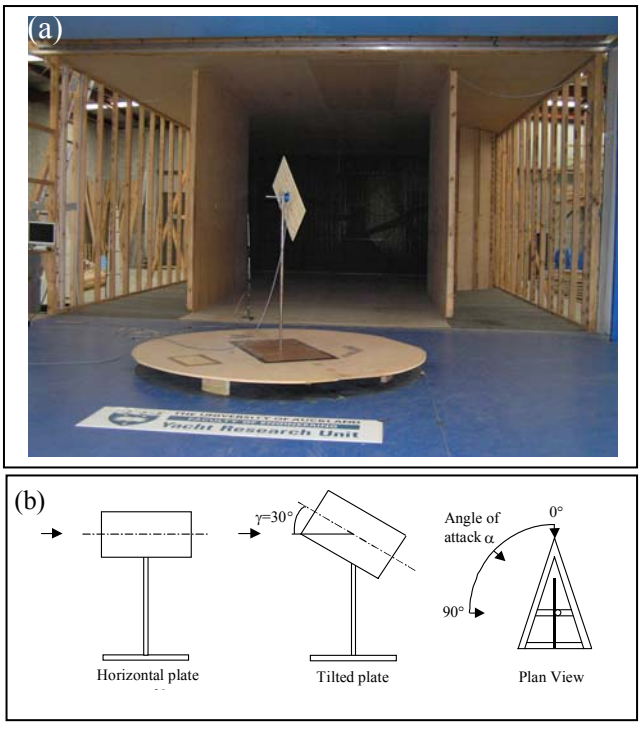

Figure 1.(a) One of the plates (SR=2) in the wind tunnel, (b) definition of the angles α and γ for the wind tunnel situation.

Forces and Moments on Plates

For plates the only significant force is that normal to the largest face (F_x). Figure 2 shows the way in which this normal force is affected by both the angle of attack and the tilt angle. For a square plate the tilt angle has very little affect and the force increases almost linearly until the plate stalls at about 35º and is almost constant thereafter. These results are similar to those presented by Holmes et al. [6], who suggest that for a square plate the normal force coefficient can be modelled by a linear variation from zero to 1.7 over the range 0-40° and a constant 1.15 at higher angles, as illustrated by the dashed line in figure 2(a). The current results do not show the very high values near 40º, which are possibly lower due to the thickness of the plate, but are very similar elsewhere.

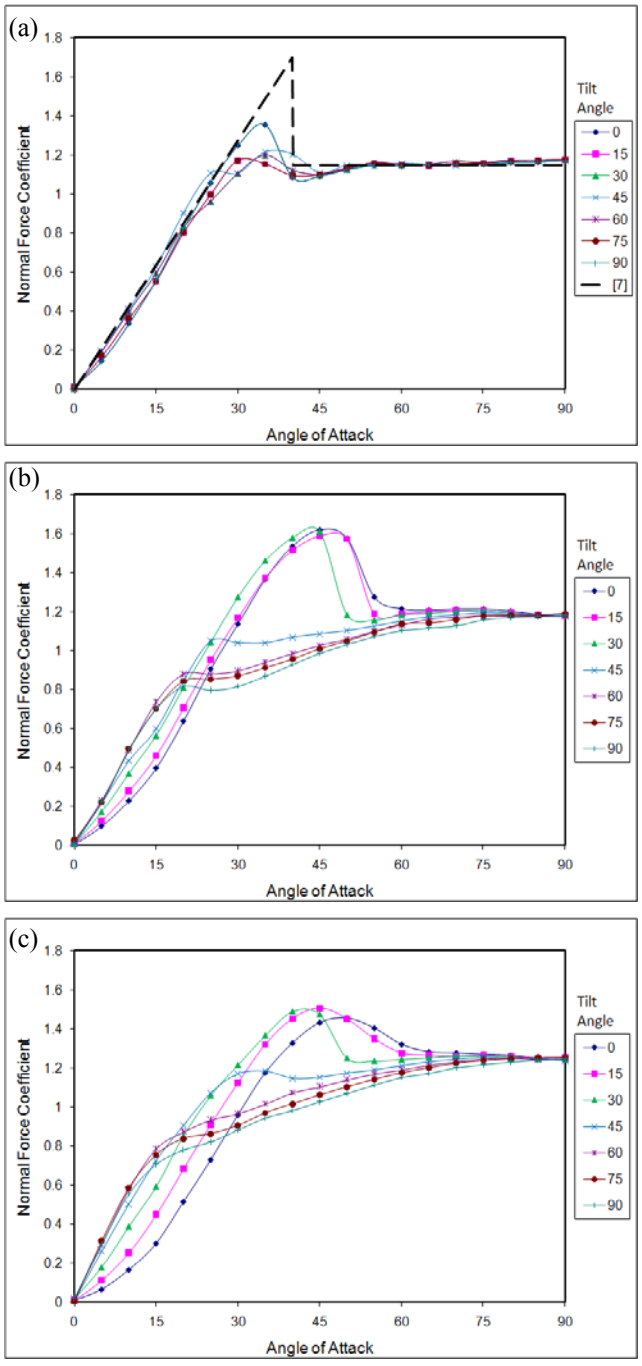

Figure 2. Normal force coefficients as a function of the angle of attack and tilt angle for plates with (a) SR =1, (b) SR=2 and (c) SR=4.

While the square plate is relatively insensitive to the tilt angle the SR=2 plate (figure 2(b)) shows quite distinct differences between the behaviour when the tilt angle $\gamma \leq 15º$ and $\gamma \geq 60°$, with the data at 30° and 45° forming a transition between the two groups. It appears that with the higher aspect ratios the initial gradient is higher but stall occurs at a lower normal force coefficient and at a lower angle of attack. The SR=4 plate (figure 2(c)) shows as

similar pattern except that the low tilt angle behaviours are not so grouped together. Analysis of the low angle of attack ($0<\alpha<5°$) gradients shows that these can be related to the aspect ratio, which is calculated from:

$$AR = SR\sin^2(\gamma) + 2\sin(\gamma)\cos(\gamma) + \cos^2(\gamma)/SR \qquad (1)$$

From simple 3D wing theory it may be expected that

$$\frac{dC_N}{d\alpha} \approx \frac{dC_L}{d\alpha} \approx \frac{2\pi}{1+2/(0.6AR)} \qquad (2)$$

where an efficiency factor of 0.6 has been included in order to approximately match the experimental data. Figure 3 shows a comparison between the measured low angle normal force coefficient gradients and equation (2).

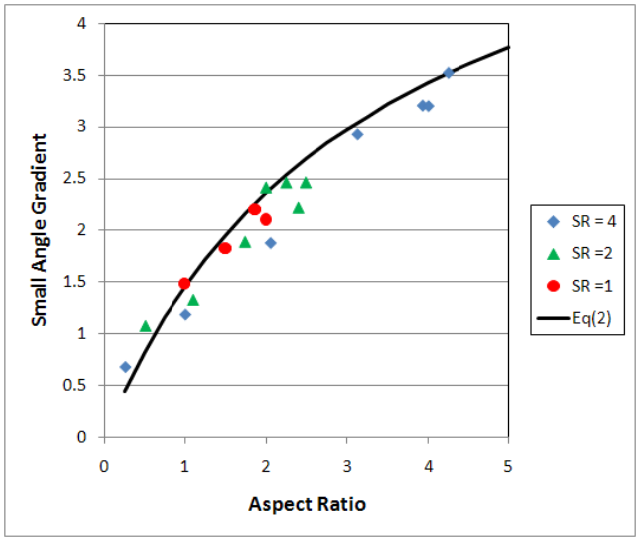

Figure 3. Small angle normal force coefficient gradients as a function of aspect ratio

The low gradients with low aspect ratios are the result of the strong downwash caused by the tip vortices. While these vortices reduce the normal force at low angles they tend to increase it at moderate angles. Smoke visualisation of the flow around the SR=4 plate at α=45° and tilt angles of γ=30 and 60° revealed quite different flow patterns. At γ=60° the flow on the leeward side of the plate is separated and while there are tip vortices these propagate downstream in the free-stream direction. In contrast at γ=60° strong "delta-wing" type vortices can be observed on the leeward side of the plate which cause the flow to wrap around the plate and deviate significantly from the free-stream direction. As a result the normal force coefficient is almost 1.5.

Even with very low aspect ratio situations the vortices become detached at sufficiently high angles of attack and the normal force coefficient becomes almost independent of both tilt and attack angles.

SR	1	2	4
C_N at =90°	1.17	1.18	1.25

Table 1. Average normal force coefficients at =90°

Table 1 shows the average measured normal force coefficients at α=90°. A small variation was observed at the various tilt angles with a typical standard deviation of 0.006. The results show a weak dependency on aspect ratio. These values are comparable with those reported by Hoerner [3] who gives values of 1.18 for a square plate and 1.21 for SR=4.

The vortices created also affect the location of the centre of pressure. As depicted in figure 4(a), where the radial lines indicate the different wind directions, for a square plate the centre of pressure is about a quarter chord windward of the centre at small angles of attack and progressively moves towards the centre as the angle of attack increases. However with the other side length ratios, while the low angle location is about a quarter chord to windward, the loci are more complex and include deviations towards the short edge of the plate, particularly with a side length ratio of 4. For trajectory modelling it has therefore been more convenient to work with the moment coefficients directly rather than working with centre of pressure locations.

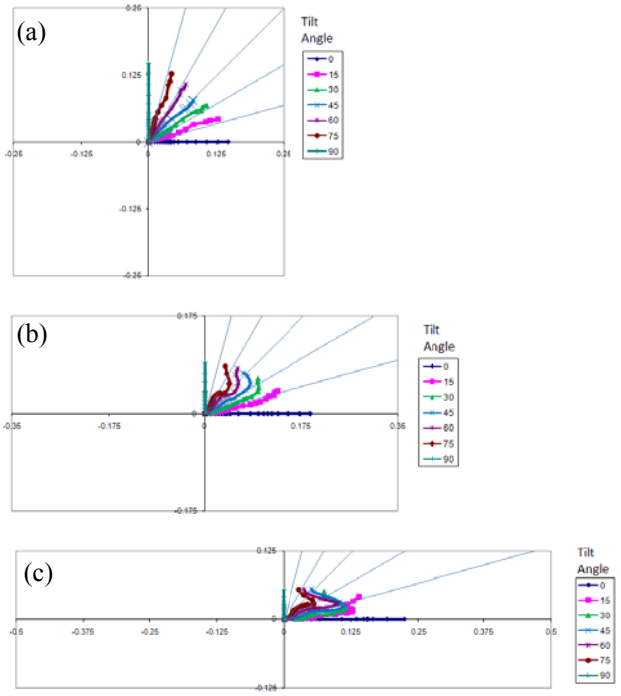

Figure 4. Centre of pressure locations for plates with side length ratios (a) 1, (b) 2 and (c) 4.

Forces and Moments on Rods

The forces and moment coefficients measured on the three rods were all fairly similar in character. As an example figure 5 shows the behaviour of the two larger force coefficients C_{Fx} and C_{Fy} for the rod with cross-section ratio CSR=2. These results show the forces to be quite complex functions of both the angle of attack and the tile angle. As might be anticipated the value of C_{Fy} when the flow is normal to that face (α=0°, γ=90°) is approximately half the value of C_{Fx} when the flow is normal to that face (α=90°, all γ), due to having only half the area while the largest face area is used to calculate the force coefficients for all faces. It may be observed in figure 5(a) that there is greater variability in the force coefficients at α=90° than occurred with the plates, this is thought to be caused by the smaller forces with rods, as a result of the smaller area, and possibly a greater sensitivity to flow variations in the tunnel due to the greater length of the rods.

One of the most noticeable differences with the rod force coefficients is the presence of conditions where either the X or Y forces are negative. This occurs when there is greater curvature in the flow, and hence lower suctions, on the more windward side face while on the more leeward side face the flow is totally separated. Such aerodynamic behaviour can lead to plunge galloping, which did occur during the earlier tests [12], which were conducted at slightly higher speeds.

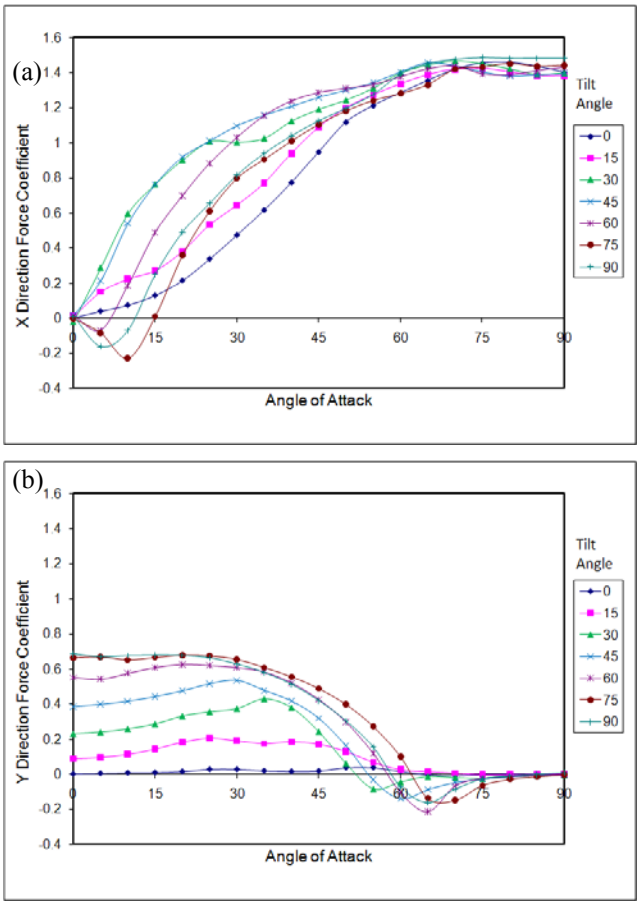

Figure 5. Major force coefficients for a rod with CSR=2, (a) C_{Fx}, (b) C_{Fy}

The moment data for the rods also showed consistent variations with both α and γ, but since these are in general created by multiple forces they cannot be interpreted in terms of centre of effort locations and hence will not be discussed in the limited space available in this paper.

Data Transfer and Interpolation

In order to transfer the data into a trajectory program and to allow interpolation each force and moment has been fitted using bi-directional short Fourier series which have been chosen to match the zeroes, symmetries and anti-symmetries of the particular force or moment function. For example the normal force coefficient is given by

$$C_{Fx} = \sum_{m=1,3,5..}^{M} \sum_{n=0,2,4,..}^{N} D_{m,n} \cos(n\gamma)\sin(m\alpha) \qquad (3)$$

where choosing M≈12 and N≈19 seemed adequate. This guarantees that the X-direction force coefficient is zero and anti-symmetric at 0°, symmetric with respect to α at 90° and -90° and symmetric with respect to γ at 0, 90, 180 and 270°.

Conclusions

Steady forces and moments have been measured on three plate and three rod geometries which represent generic examples of windborne debris. It has been shown that these forces and moments are complex functions of the angle of attack, the tilt angle and the geometry. With plates some of the characteristics can be related to the effective aspect ratio for a particular orientation. Methods for transferring the data into a trajectory program and allowing interpolation have been outlined.

References

[1] Baker, C.J., "Solutions of the debris equations", *6th UK Conf. on Wind Eng., Cranfield, 15-17 September 2004.*

[2] Baker C.J., "The debris flight equations", *J. Wind Eng. Ind. Aerodyn*. **95**, 2007, 329-353.

[3] Hoerner, S.F., *Fluid-Dynamic Drag*. Hoerner Fluid Dynamics, USA. 1965.

[4] Holmes, J.D., "Trajectories of spheres in strong winds with application to wind-borne debris", *J. Wind Eng. Ind. Aerodyn.* **92**, 2004, 9-22.

[5] Holmes, J.D. & English, E.C., "Aerodynamics and trajectories of windstorm debris. Part 2. Sheet objects". *11th AWES Workshop*, Darwin, Australia, 28-29 June 2004.

[6] Holmes, J.D., Letchford, C.W. and. Lin, N., "Investigation of plate-type windborne debris. Part II. Computed trajectories", *J. Wind Eng. Ind. Aerodyn.*. **94**, 2006, 21-39.

[7] Flachsbart, O.," Messungen an ebenen und gewolbten Platten", Ergebnisse der AVA, IV. 1932.

[8] Lin, N., Letchford, C.W. & Gunn, T., "Investigation of flight mechanics of 1D (rod-like) debris", The Fourth European & African Conf. on Wind Eng., Prague, 11-15 July, 2005, Paper #300.

[9] Lin, N., Letchford, C.W. & Holmes, J.D., "Investigation of 2D wind-borne debris in wind-tunnel and full scale tests". *11th AWES Workshop*, Darwin, Australia, 28-29 June 2004.

[10] Lin, N., Letchford, C.W. & Holmes, J.D. (2006), "Investigation of plate-type windborne debris. Part I. Experiments in wind tunnel and full scale", *J. Wind Eng. Ind. Aerodyn*. **94**, 2006, 51-76.

[11] Richards, P.J., Williams, N., & Laing, B., "3-Dimensional aerodynamics and motion of plate type wind-borne debris", *6th Asia-Pacific Conf. on Wind Eng., Seoul, Korea, 12-14 September 2005, 762-777.*

[12] Richards, P.J., Williams, N., Laing, B., McCarty, M. & Pond, M., "Numerical Calculation of the 3-Dimensional Motion of Wind-borne Debris", *J. Wind Eng. Ind. Aerodyn*., **96**, 2008, 2188-2202.

[13] Tachikawa, M. & Harra. H., "Trajectories and velocities of typhoon-generated missiles, Part 3 Aerodynamic characteristics of various missile shapes", *Proc. of Transactions of the Architectural Institute of Japan*, No.319, 1982, 23-31.

[14] Tachikawa, M., " Trajectories of flat plates in uniform flow with application to wind-generated missiles". *J. Wind Eng. Ind. Aerodyn.*, **14**, 1983, 443 – 453.

[15] Tachikawa, M., "A method for estimating the distribution range of trajectories of wind borne missiles". *J. Wind Eng. Ind. Aerodyn*., **29**, 1988, 175 – 184.

[16] Visscher, B.T. & Kopp, G.A., "Trajectories of roof sheathing panels under high winds", *J. Wind Eng. Ind. Aerodyn.*, **95**, 2007, 697-713.

[17] Wang, K. & Letchford, C.W., "Flying Debris Behaviour", *11th Int. Conf. on Wind Eng.*, Lubbock. Texas, 2003.

[18] Wills, J.A.B., Lee, B.E. and Wyatt, T.A., "A model of wind-borne debris damage". *J. Wind Eng. Ind. Aerodyn.* **90**, 2002, 555 – 565.